ELSEVIER

Journal of Nuclear Materials 251 (1997) 123–131

journal of nuclear materials

Atom transport under ion irradiation

P. Fielitz, M.-P. Macht, V. Naundorf *, H. Wollenberger

Hahn-Meitner-Institut Berlin, Glienickerstr. 100, 14109 Berlin, Germany

Abstract

Diffusion coefficients in nickel single crystals under heavy ion irradiation were measured near the irradiated surface by using multi-layer specimens. Analysis of the depth dependence of these diffusion coefficients yields information on the effective fraction η of the displacement rate, with which transporting, i.e., 'freely migrating' defects are produced, and on the radiation-induced sink strength. Upper limits of $\eta = 7\%$ are estimated for a self-ion irradiation at 950 K. By increasing the irradiation temperature from 800 to 950 K the effective sink strength was observed to decrease while η increases. The relation between swelling rates and the magnitude of the radiation-enhanced diffusion coefficient is briefly discussed.

1. Introduction

Energetic ions are frequently used in order to study the irradiation effects in structural materials of fission and fusion reactors. These irradiation effects include microstructural changes in the material, e.g., void formation, which is responsible for the dimensional instability, or phase transformations, which may degrade the mechanical properties. The origin of the microstructural changes is the radiation-induced diffusion [1]. It is one of the aims of radiation damage modelling to understand the relation between the defect production process under cascade forming irradiation conditions and the long-range atom transport so that valid predictions of transport effects can be made for arbitrary irradiation conditions including the technically important case of neutron irradiation.

Atom transport under irradiation arises generally from both, relocation of the knock-on atoms and thermally activated migration of the radiation-induced point defects. The former process is also known as atomic mixing [2]. It is rather efficient for cascade forming ion irradiation and is the dominating transport effect at low temperatures where thermally activated jumps of atoms are inhibited. The random displacements of atoms in the collision cascade suggest a description for the mixing effect in terms of a diffusion coefficient, D_{mix}, which is expected to be proportional to the displacement rate per atom, K (in units of displacements per atom per second, dpa/s). Typical values of the mixing efficiency D_{mix}/K of about 1 nm^2/dpa are experimentally observed for 300 keV Ni^+ ion irradiation of nickel in the peak damage region [3]. At elevated temperatures radiation-induced point defects contribute to transport according to their concentration and mobility. For example, the diffusion coefficient D_{rad} of the radiation-enhanced self-diffusion is given by $D_{rad} = f_v D_v C_v + f_i D_i C_i$ + (additional terms) [1]. Here f is the correlation factor, D is the diffusion coefficient, and C is the concentration of transporting defects. The subscripts v and i indicate single vacancies and interstitial atoms, respectively, and the terms within the brackets allow for further (generally small) contributions arising from mobile defect clusters [1,4]. Since the point defects are produced in excess of their thermal equilibrium concentration by the irradiation they tend to annihilate either by recombination or at defect sinks, e.g., at external surfaces or at microstructural lattice disturbances like dislocations or phase boundaries. Consequently the magnitude of the radiation-enhanced diffusion under steady state irradiation conditions is determined by the dynamical equilibrium between the production and annihilation rates of the point defects [1]. Hence a knowledge of these rates is required for realistic damage modelling.

The interpretation of measurements of the radiation-enhanced diffusion caused by cascade forming ion irradiation

* Corresponding author. Tel.: +49-30 8062 2765; fax: +49-30 8062 3059.

0022-3115/97/$17.00
PII S0022-3115(97)00220-1

with respect to defect production and annihilation rates is considerably impeded by two specific properties of this type of radiation damage: (i) simultaneous production of mobile point defects and of an immobile microstructure, which acts as defect sink, and (ii) damage production restricted to a volume near to the irradiated surface. The first property has been discussed to some detail for the steady state irradiation conditions [3–5]. On the basis of available diffusion data it was concluded that the production rate of transporting defects is only of the order of a few percent of the displacement rate. This estimate depended on the type of ion used for the irradiation and the sink strength estimated from microstructural observation [4,6]. In particular the determination of the effective sink strength and its temperature and displacement rate dependence turned out to be difficult. For example, it became evident that estimates of the ion-induced sink strength determined by electron microscopic investigations are probably only lower limits of the actual ones. On the other hand, the possible influences of the surface and of the inhomogeneous damage distribution on the magnitude of the transport effect were not considered in this discussion, mainly because experimental data were not available.

In this communication the radiation-enhanced diffusion near the irradiated surface is analyzed and spatially resolved measurements of the self-diffusion coefficients of ion irradiated nickel are presented. The well known effect of the surface sink on the spatial variations of the mobile defect concentrations [1] and the limited range of the ion-induced damage together with the known defect properties [7] will be used to estimate both, the effective production rate of transporting defects and the effective sink strength at temperatures around the swelling rate maximum.

2. Experimental details

Two types of nickel multi-layer specimens were used in the present investigation. The first type was grown on a sapphire substrate 12×12 mm^2 wide covered with about 300 nm of nickel. Repeating five times an alternate sputter deposition about 1 nm of cobalt and vapor deposition of about 50 nm nickel with a purity of 5N five layer specimens were produced where the first cobalt layer was situated about 50 nm below the irradiated surface. The other type was grown on a well polished Ni single crystal with a diameter of 12 mm cut about 5° off the (112) zone axis. These specimens contained four thin layers of about 1 nm of the ^{63}Ni tracer about 100 nm apart starting with the first layer about 100 nm below the irradiated surface. For some experiments single crystal specimens with only one tracer layer in a depth of about 75 nm below the irradiated surface were produced. All the specimens were prepared under UHV conditions at room temperature. Electron microscopic investigation showed that the specimens grown on the sapphire substrate were polycrystalline with a grain size of about 50 nm, while the layer structures grown on the single crystals had the orientation of the base crystal.

Only part of the specimens' surface was irradiated with 600 keV Kr^{2+} and 300 keV Ne^+, Ar^+ and Ni^+ ions through an appropriate aperture of about 0.2 cm^2. This procedure allowed to analyze the irradiated and not irradiated state on one and the same specimen so that the irradiation effect could be evaluated with high accuracy by comparison [3]. Irradiations at and below room temperature were performed on specimens grown on the sapphire substrate, while irradiations at and above 800 K were performed on the single crystal sandwich specimens. It was expected that at the higher irradiation temperatures thermally activated defect migration is the leading transport effect while at the lower irradiation temperatures the ion mixing dominates the transport. Since Ni and Co are neighbors in the periodic table and their diffusion behavior is quite similar [8] atomic mixing of Co in nickel should represent that of the nickel matrix itself [2].

The depth dependent displacement cross-section $\sigma_d(x)$ of the different irradiating ions in nickel was calculated by means of the binary collision code TRIM [9] using a threshold energy of 40 eV [10]. Values of $\sigma_{d,max}$, the displacement cross-section in the damage maximum are compiled in Table 1 together with the characteristic depth L of the damaged region, $L = \int dx\, \sigma_d(x)/\sigma_{d,max}$. The depth dependent displacement rate $K(x)$ in dpa/s is obtained from the ion flux density φ in the usual way as $K(x) = \varphi\sigma_d(x)$.

Atom transport was measured from the broadening of the thin tracer layers by sectioning using sputter erosion by 4 keV O_2^+ ions with a current density of about 400 mA/m^2 in combination with secondary ion mass spectrometry (SIMS). Details of this measuring technique are reported elsewhere [3]. As an example, Fig. 1 presents the concentration depth profiles of ^{63}Ni as measured before and after 300 keV Ne^+ irradiation at 950 K on the same single crystal. The ion flux density was 3×10^{17} ions m^{-2} s^{-1} and the irradiation time 250 s. Instrumental depth resolution of 12 nm at a depth of about 110 and 20 nm at a depth of about 460 nm, arising from atomic mixing and roughening during sputter erosion [11] is obvious in the profile obtained in the as-prepared condition (open circles). The effect of thermal diffusion is visible in the depth

Table 1
Maximum displacement cross-section, $\sigma_{d,max}$, and characteristic depth, L, of the damaged region in nickel according to TRIM [9] for irradiation with different ions

	600 keV Kr^{2+}	300 keV Ne^+	300 keV Ar^+	300 keV Ni^+
$\sigma_{d,max}$ (nm^2)	0.26	0.041	0.11	0.20
L (nm)	139	240	142	95

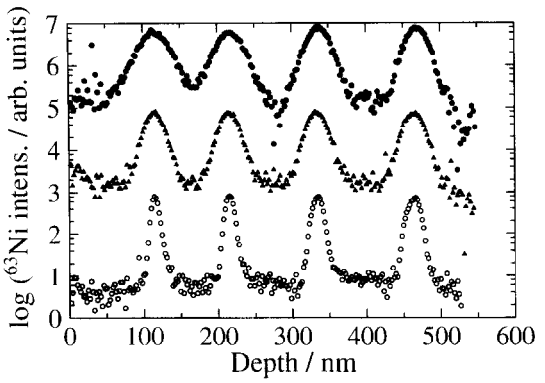

Fig. 1. ^{63}Ni intensity of a ^{63}Ni/Ni multi-layer specimen as measured by means of SIMS. Lower curve: as prepared; center curve: thermal treatment during irradiation time at 950 K; upper curve: 300 keV Ne^+ irradiation at 950 K. The different curves are shifted along the intensity axis by arbitrary amounts.

profile obtained after irradiation in the non-irradiated part of the specimen (closed triangles), while the depth profile obtained in the irradiated part (closed circles) shows the combined effect of three contributions, thermal diffusion, radiation-enhanced diffusion, and atomic mixing. In terms of the effective diffusion coefficient under irradiation, D_{irr}, it is assumed that $D_{\mathrm{irr}} = D_{\mathrm{therm}} + D_{\mathrm{rad}} + D_{\mathrm{mix}}$ is valid.

Effective diffusion coefficients were derived from the variance of each of the layers in the different depths by fitting a Gaussian curve to the respective peak. The central portion of the peak covering a concentration variation of more than one order of magnitude was used for the fitting procedure. If σ^2 is the variance of the Gaussian curve measured after irradiation on the irradiated part of the specimen and σ_0^2 that measured on the non-irradiated part, then the irradiation-induced diffusion coefficient is calculated as $D_{\mathrm{rad}} + D_{\mathrm{mix}} = (\sigma^2 - \sigma_0^2)/2t$, where t is the irradiation time. Since the diffusion coefficient of atomic mixing was measured independently by a low temperature irradiation experiment for the different ions the radiation-enhanced diffusion coefficient could be determined by the difference between the respective measurements at the same depth. Generally three SIMS measurements in the irradiated and the non-irradiated region were used to evaluate the diffusion coefficients. The error bar of these values is about $\pm 30\%$.

3. Radiation-enhanced diffusion near the plane surface

The radiation-enhanced diffusion is essentially caused by the radiation-enhanced concentration $C_{\mathrm{i,v}}$ of mobile single interstitials and vacancies (subscript i and v, respectively) while mobile agglomerates contribute only little [4,5]. During homogeneous irradiation of an infinitely extended crystal these defect concentrations are determined by the dynamical equilibrium of defect production and annihilation rates at distributed sinks alone. In the case of heavy ion irradiation they are also determined by diffusion due to defect gradients which arise because of the presence of the surface sink, where the defect concentrations are assumed to be always in thermal equilibrium, and because of depth dependent defect production rates and sink strengths. Because the defects can migrate away from the location where they were produced it is in particular expected that considerable defect concentrations will build up in parts of the crystal beyond the ion range, i.e., in parts which were not directly damaged by the irradiating ions.

For cascade forming irradiation the primary production consists of defect agglomerates and only to a small fraction of single defects [12]. Since the fractions of agglomerated vacancies and interstitials generally are not equal it must be assumed that the single defects are also produced with different effective fractions $\eta_{\mathrm{i,v}}$ of the depth dependent displacement rate $K(x)$. Defect annihilation may occur by mutual recombination of vacancies and interstitials, and at a sink structure as given by the radiation-induced microstructure of loops and voids or at interfaces. Since the annihilation by recombination is only relevant for high and nearly equal production rates of single defects and low sink strength [1] it can be neglected under cascade forming irradiation conditions at elevated temperatures [4]. The effective sink strengths for interstitials and vacancies, $k^2_{\mathrm{i,v}}(x)$, are different because of the annihilation bias [13]. Hence, considering the linear diffusion problem near the plane surface, the radiation-enhanced point defect concentrations for steady state conditions are given by [1,4]

$$D_{\mathrm{i,v}} \Delta C_{\mathrm{i,v}} + \eta_{\mathrm{i,v}} K(x) - k^2_{\mathrm{i,v}}(x) D_{\mathrm{i,v}} C_{\mathrm{i,v}} = 0, \qquad (1)$$

with the boundary condition of $C_{\mathrm{i,v}} = 0$ at the irradiated surface and at very large distance from it in the region of negligible defect production. Steady state of the defect concentrations are obtained as soon as the slowest defect (in nickel this is the vacancy [7]) after production has reached its sink, i.e., after irradiation times larger than the relaxation time $\tau = 1/(k_{\mathrm{v}}^2 D_{\mathrm{v}})$ of annihilation of the vacancies [1].

The steady state self-diffusion coefficient, D_{rad}, is given by the sum of contributions from the interstitial and vacancy fluxes [1] and obeys a diffusion equation similar to Eq. (1),

$$\Delta D_{\mathrm{rad}}(x) + \eta K(x) - k^2(x) D_{\mathrm{rad}}(x) = 0, \qquad (2)$$

with an effective fraction $\eta = (f_{\mathrm{i}}\eta_{\mathrm{i}} + f_{\mathrm{v}}\eta_{\mathrm{v}})$ of the mobile single defect production rate and an effective sink strength k^2, which is defined as the average of the sink strengths k_{i}^2 and k_{v}^2 in the form of $k^2 = (f_{\mathrm{i}} k_{\mathrm{i}}^2 D_{\mathrm{i}} C_{\mathrm{i}} + f_{\mathrm{v}} k_{\mathrm{v}}^2 D_{\mathrm{v}} C_{\mathrm{v}})/D_{\mathrm{rad}}$. Since the annihilation bias of the microstructure for the interstitials and vacancies is expected to be small [4], in the following $k_{\mathrm{i}}^2 \approx k_{\mathrm{v}}^2 \approx k^2$ will be assumed.

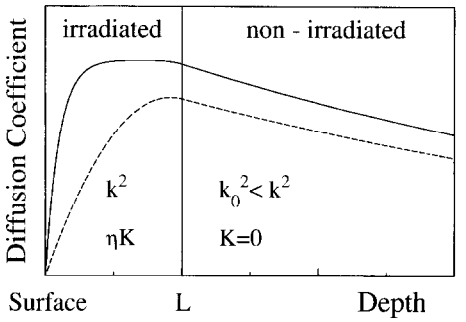

Fig. 2. Schematic presentation of the depth dependent diffusion coefficient according to Eq. (2) of the text. Constant defect production rate ηK and sink strength k^2 are assumed between the irradiated surface and depth L, sink strength $k_0^2 < k^2$ and no defect production are assumed at a depth larger than L. The two profiles represent the limiting cases of high sink strength ($kL > 1$, solid line) and low sink strength ($kL < 1$, dashed line) according to Eq. (4) of the text.

Due to the depth dependence of the production rate and the sink strength in Eq. (2) the diffusion coefficient D_{rad} can be evaluated only numerically. However, its general behavior is easily discussed for the special case that the damage is confined to a depth L below the irradiated surface, where the defect production rate and the sink strength are constant with values of ηK and k^2, respectively. Beyond the depth L the defect production rate is assumed to be zero and the sink strength k_0^2 to be lower than in the irradiated region, i.e., $k_0^2 < k^2$. In Fig. 2 this situation is illustrated. In the region of negligible defect production beyond the depth L Eq. (2) predicts an exponential slope of the diffusion coefficient, i.e.,

$$D_{\text{rad}} = \text{const}\exp(-k_0 x) \quad \text{if } x > L. \tag{3}$$

Hence, diffusion measurements in this region will result in the determination of the effective sink strength of the non-irradiated crystal without any assumption on the defect production rate.

Within the ion range L the diffusion coefficient has a maximum of magnitude

$$D_{\text{rad,max}} = \begin{cases} \eta K/k^2, & \text{if } kL > 1, \\ \eta K L^2, & \text{if } kL < 1, \end{cases} \tag{4}$$

indicating that the surface sink has a negligible influence if the defect absorption length $1/k$ of the microstructure is smaller than the depth L of defect production. In this case the defects annihilate rather at the microstructure than at the surface and the maximum diffusion coefficient is given by the well known relation derived for homogeneous irradiation. A measurement of the maximum diffusion coefficient would provide then only the ratio of defect production and annihilation rates [1,4]. If on the other hand the defect absorption length is larger than the depth of defect production, $1/k > L$, then the maximum diffusion coefficient is independent of the actual sink strength and the fraction of mobile defect production η can be directly evaluated from a measurement of $D_{\text{rad,max}}$.

In contrast to the case of homogeneous irradiation a measurement of the depth dependence of the diffusion coefficient can provide information on both, the fraction of mobile defect production and of the sink strength. For example, with Eq. (2) the relation

$$D(0)'^2 \le \eta K D(L) \le 2D(0)'^2 \tag{5}$$

is valid which indicates that knowledge of the slope of the diffusion coefficient at the surface, $D(0)'$, and its value at the end of the damaged region, $D(L)$, already yields an estimate of the effective fraction of mobile defect production. This could then be used in Eq. (4) for an estimate of the proper sink strength. In fact, because the sink strength and the production rate act differently on the diffusion coefficient in different depths, a fit of Eq. (2) to actual measurements of the radiation-enhanced diffusion coefficient D_{rad} will yield independent estimates of the effective sink strength and mobile defect production rates for realistic irradiation conditions.

4. Results and discussion

Measurements of the depth dependent diffusion can be interpreted by Eq. (2) only when three items have been analyzed before: (i) steady state irradiation conditions, (ii) depth dependence of the defect production, and (iii) depth dependence of the sink strength. Steady state conditions have been verified experimentally at temperatures of 800 and 950 K for 600 keV Kr^{2+} and 300 keV Ni^+ irradiation with displacement rates of 1.15×10^{-2} dpa/s and 2.74×10^{-3} dpa/s, respectively. Fig. 3 displays the diffusional broadening in terms of $D_{\text{rad}}t$ as a function of fluence. The

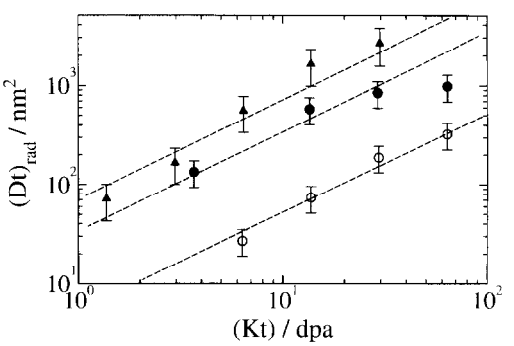

Fig. 3. Dependence of the diffusional broadening $D_{\text{rad}}t$ on fluence in a double-logarithmic plot. Open and closed circles: 600 keV Kr^{2+} irradiation at 800 and 950 K, respectively. The broadening was measured at a depth of 80 nm, the displacement rate was 1.1×10^{-2} dpa/s. Filled triangles: 300 keV Ni^+ irradiation at 950 K. The broadening was measured at a depth of 55 nm, the displacement rate was 2.7×10^{-3} dpa/s. The dashed lines indicate slope one.

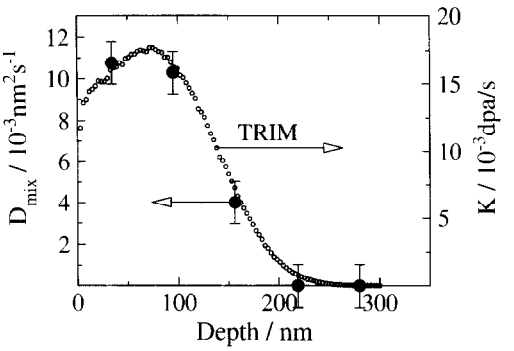

Fig. 4. Comparison of measured mixing coefficients (data points with error bars) with calculated displacement rates vs. depth (600 keV Kr^{2+}, 6.8×10^{16} m^{-2} s^{-1}, 4850 s at 77 K).

linear relation indicates that the radiation-enhanced diffusion coefficient is independent of time at the displacement rates, fluences and temperatures given. This in turn points not only at a time independent mobile defect concentration but also at a stable microstructure for fluences larger than 1 dpa, which is in accordance with electron microscopic investigations [14,15].

The depth dependence of the defect production under ion irradiation is usually assumed to follow the spatial variations of the displacement cross-section, which can be calculated for instance with a simulation program like TRIM [9]. The validity of this assumption has been verified by measuring the depth dependence of the diffusion coefficient under irradiation at 77 K. At these temperatures

Table 2
Mixing efficiencies in nickel irradiated with different ions at 77 K in units of nm^2/dpa

	600 keV Kr^{2+}	300 keV Ne^+	300 keV Ar^+	300 keV Cu^+
D_{mix}/K	0.67 ± 0.12	0.42 ± 0.08	0.56 ± 0.09	0.49 ± 0.07

the diffusivity is determined by atomic mixing [2] and therefore it maps the displacement rate. In Fig. 4 the calculated displacement rate and the measured diffusion coefficients for a 600 keV Kr^{2+} irradiation are compared. A mixing efficiency of $D_{mix}/K = 0.67 \pm 0.12$ nm^2/dpa is derived independent of depth for the measurements within the first 200 nm below the surface. Beyond this depth no diffusive broadening of the layers could be resolved because it was smaller than the detection limit of the measuring technique. A similarly good agreement between calculated depth dependent displacement rates and measured diffusion coefficients was observed for a 300 keV Cu^+ irradiation at 77 K. The latter result may be regarded as that of a self-ion irradiation of nickel, since the masses are similar. The mixing efficiencies obtained for the ions used in this investigation are compiled in Table 2.

The depth dependence of the effective sink strength is only incompletely known. Certainly the sink strength k_0^2 valid in the region not damaged by the ions is expected to be lower than k^2, the effective value in the damaged region. Lower limits of the sink strength of $k^2 = 10^{15}$ m^{-2}

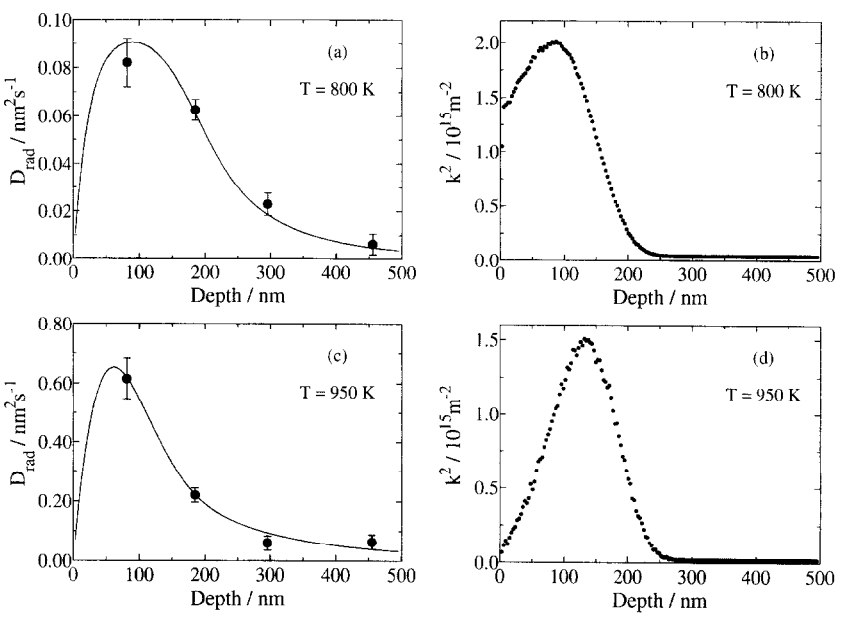

Fig. 5. Depth dependence of the radiation-enhanced diffusion coefficients obtained after a 300 keV Ar^+ irradiation at (a) 800 K, 2.5×10^{17} m^{-2} s^{-1}, 520 s; and (c) 950 K, 2.7×10^{17} m^{-2} s^{-1}, 280 s. The solid lines are fits of a solution of Eq. (2) of the text to the data points using the sink strengths shown in (b) and (d), respectively.

were deduced in the damaged region from the observed microstructure of self-ion irradiated nickel at temperatures of 800 to 850 K [3]. Quite similar values were found in dual-beam (300 keV Ni^+ and 25 keV He^+) irradiated stainless steel at 800 K [16]. In the peak damage region of 180 keV Kr^+ ion irradiated nickel at 773 K the sink strength of the bubbles which form after a fluence of about 20 dpa is estimated to $k^2 = 10^{16}$ m^{-2} [17]. Results obtained for room temperature low fluence He^+ ion irradiations indicate that loops are formed in the whole penetration range of the ions, while at temperatures of 820 K a near surface region of considerably reduced loop density is observed [18,19]. The latter result is supported by the observation of a 30 nm thick surface layer of reduced cavity density after dual-beam irradiation of stainless steel [16]. These sparse informations suggest a depth distribution of the effective sink strength evolving under displacement damage according to the depth dependence of the displacement cross-section. Thus for all self-ion irradiations and for noble gas irradiations at lower temperatures

$$k^2 = k_0^2 + k_{max}^2(\sigma_d(x)/\sigma_{d,max}) \quad (6a)$$

is assumed, where the maximum sink strength k_{max}^2 may include a possible temperature and displacement rate dependence. At higher temperatures where small dislocation loops become thermally unstable irradiation with noble gases can result in a relatively stable bubble microstructure [19]. Hence under noble gas irradiation at elevated temperatures the sink structure can be expected to be dominated by the depth distribution $p(x)$ of the implantation profile [19], namely,

$$k^2 = k_0^2 + k_{max}^2(p(x)/p_{max}). \quad (6b)$$

The present results will be interpreted under the assumption that the sink strength follows the depth dependence of the displacement cross-section (Eq. (6a)) for all self-ion irradiations and for irradiation with noble gases at 800 K. The sink strength produced by the noble gas irradiation at the higher temperature of 950 K is assumed to follow the depth distribution of the implantation (Eq. (6b)). With these assumptions a fit of Eq. (2) to the depth dependent measurements, which will be discussed next, determines the three parameters effective fraction of transporting defects, η, maximum effective sink strength in the irradiated region, k_{max}^2, and effective sink strength in the non-irradiated region, k_0^2.

Fig. 5a and c show data of the radiation-enhanced diffusion coefficient as obtained for a 300 keV Ar^+ irradiation at 800 and 950 K, respectively. The solid curves are fits of Eq. (2) to the data using the depth dependent sink strengths according to Eqs. (6a) and (6b) which are presented in Fig. 5b and d, respectively. Fits of Eq. (2) to the data obtained for 300 keV Ne^+ and Ni^+, and for 600 keV Kr^{2+} irradiation are shown in Fig. 6a–c. The exponential slope of D_{rad} beyond the damaged region, which is predicted by Eq. (3) and which arises from the mobile defect

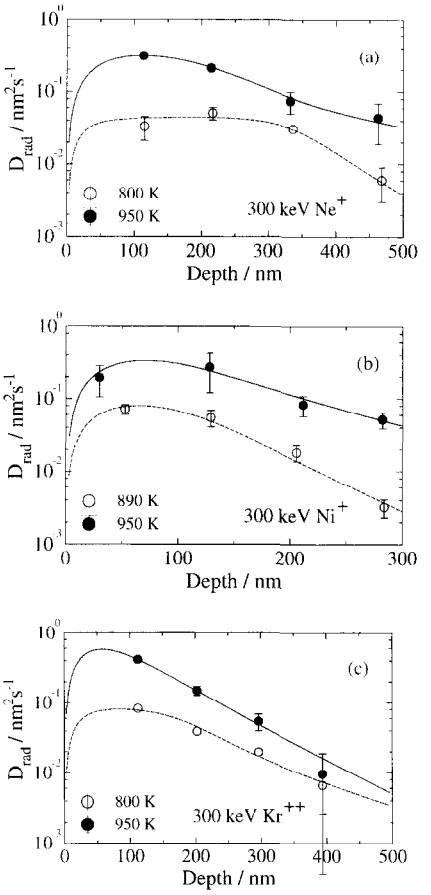

Fig. 6. Semilogarithmic plots of the depth dependence of the radiation-enhanced diffusion coefficients after irradiation. (a) 300 keV Ne^+, 3.0×10^{17} m^{-2} s^{-1} (800 K: 435 s; 950 K: 250 s); (b) 300 keV Ni^+ (890 K: 1.9×1016 m^{-2} s^{-1}, 2000 s; 950 K: 1.4×10^{16} m^{-2} s^{-1}, 500 s); (c) 600 keV Kr^{2+}, 6.8×10^{16} m^{-2} s^{-1} (800 K: 270 s; 950 K: 280 s). The solid lines are fits of a solution of Eq. (2) of the text to the data points.

concentration there, is obvious in these semi-logarithmic plots. From these slopes the sink strengths k_0^2 are obtained, which are between 0.5×10^{14} and 3.5×10^{14} m^{-2} at the irradiation temperature of 800 K, and between 0.2×10^{14} and 1.5×10^{14} m^{-2} at the higher temperature of 950 K. These sink strengths decrease slightly with increasing temperature and they are higher than those expected for a well annealed single crystal. It may be speculated whether the long range, one-dimensional glide of small interstitial loops [20] out of the irradiated region and accumulation of these in the non-irradiated region is responsible for this effect.

Fig. 7 presents the effective production rates of transporting defects, η, and the effective sink strengths, k_{max}^2, deduced from the measurements shown in Figs. 5 and 6. Obviously, the effective production rates of transporting defects, η, cluster around about 1% to 2%. This low value

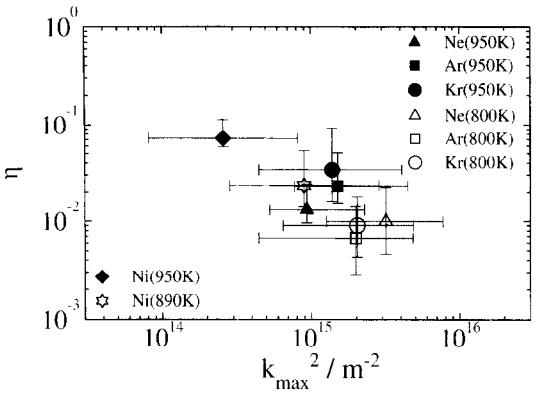

Fig. 7. Effective fraction of transporting defects, η, vs. the maximum sink strength, k^2_{max}, for the irradiation conditions indicated.

is in general accordance with earlier results [3,6]. Only for the self-ion irradiation performed at 950 K a higher effective production rate of about 7% was observed. Taking properly into account the effect of the surface sink in a re-evaluation of earlier diffusion experiments performed at the same temperature [3] this high value is also obtained.

The sink strength k^2_{max} in the irradiated region decreases with increasing temperature quite similar to the behavior of the sink strength k^2_0 in the non-damaged region. For the self-ion irradiations this temperature dependence is particularly large, while the effect under noble gas irradiation is smaller, probably because noble gas bubbles are relatively stable. The correlation observed in Fig. 7 between η and k^2_{max} may be explained by the thermal instability of small vacancy clusters at higher temperatures, which not only should lower the effective sink strength at these temperatures but also would yield an enhanced production rate of vacancies. This would obviously result also in different effective production rates of vacancies and interstitials, as was already assumed above when writing down Eq. (1).

A possible displacement rate dependence of the effective sink strength is expected to show up in the respective dependence of the radiation-enhanced diffusion coefficients. Fig. 8a and b present the results obtained under noble gas irradiation at 800 and 950 K. Here the displacement rate dependence was investigated near the maximum of the depth dependent damage rate by using mono-layer specimens. Since by the noble gas irradiation a sink strength larger than $k^2 = 10^{15}$ m^{-2} is induced (cf. Fig. 7), the absorption length of defects is smaller than the characteristic depth L of the damage profile (cf. Table 1) and $kL > 1$ applies. Hence, according to Eq. (4), the surface sink may be neglected and the data shown in Fig. 8a and b are representative of a homogeneous irradiation performed in the sink annihilation regime of defect reactions. The linear relation obtained under irradiation at 800 K (cf. Fig. 8a) then indicates, that $\eta/k^2 =$ const., i.e., independent of the displacement rate, while at 950 K η/k^2 decreases slowly with increasing displacement rate (cf. Fig. 8b). Furthermore, η/k^2 is higher at 950 than at 800 K, in accordance with the results shown in Fig. 7. Since the production rate of transporting defects should be proportional to the displacement rate, i.e., η should be independent of the displacement rate, it is concluded that the sink strength at 800 K is also independent of it, while at 950 K the sink strength increases with increasing displacement rate. TEM investigations of the temperature dependence of the microstructure after self-ion irradiation with displacement rates of 7×10^{-2} and 7×10^{-4} dpa/s [21] indicated that the sink strength at 800 K is more than one order of magnitude higher than at 950 K. Moreover, the sink strength at 800 K decreased by a factor of four when the displacement rate was decreased by two orders of magnitude. At the higher temperature of 950 K an even higher decrease of the sink strength by more than one order of magnitude was observed for the same variation of the displacement rate [21]. The present investigation indicates a considerably weaker dependence. This may be due not only to the noble gas instead of the self-ion irradiation, but also to the different kinds of experiments: while conven-

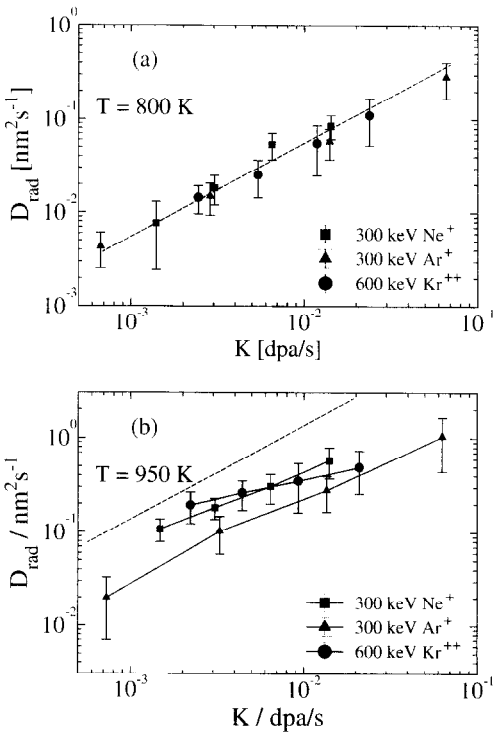

Fig. 8. Dependence of the radiation-enhanced diffusion coefficients on the displacement rate measured at a depth of about 75 nm for irradiation with noble gases at (a) 800 K (Ne^+: 3.4 dpa; Ar^+: 6.2 dpa; Kr^{2+}: 6.4 dpa) and (b) 950 K (Ne^+: 1.7 dpa; Ar^+: 2.9 dpa; Kr^{2+}: 3.7 dpa). Slope one is indicated as dashed line in (a) and (b), respectively.

tional TEM investigations are performed at room temperature after the irradiation was finished, the presently reported parameters represent the situation during irradiation at the corresponding temperature. Theoretical investigations aiming at a deeper understanding of the temperature and displacement rate dependence of the effective sink strength, and its relation to the effective production rate of transporting defects for cascade forming irradiation conditions at high temperatures and fluences are necessary before more quantitative interpretations are possible [22].

Recently, the magnitude of η has been discussed with respect to the swelling phenomenon [4]. Swelling occurs when the flux of vacancies into voids exceeds that of interstitials. Large swelling rates $\mathring{S}$ are in particular expected in cases when the majority of the interstitials annihilate at sinks different from the voids [4,20]. In any case the actual swelling rate is a lower bound of the vacancy flux into the voids including single vacancies as well as mobile vacancy clusters. The agglomerates contribute only little to diffusion [4,5]. If they would contribute also little to swelling then the relation [4]

$$\mathring{S}/K \leq \eta^* k_c^2/k^2 \leq k_c^2 D_{\mathrm{rad}}/K \tag{7}$$

is valid, where $\eta^* K$ is the effective production rate of single vacancies, and k_c^2 is the effective sink strength of the voids. Obviously Eq. (7) is a useful 'compatibility test' between swelling and diffusion data: failure of the test indicates a significant contribution of vacancy clusters to swelling.

Peak swelling rates at 823 K of $\mathring{S}/K = 1.9 \times 10^{-3}$ have been reported for a nickel self-ion irradiation with a displacement rate of 7×10^{-4} dpa/s [21]. The sink strength of voids in this experiment was determined to be $k_c^2 = 1.9 \times 10^{14}$ m^{-2}, the total sink strength to be $k^2 = 3 \times 10^{14}$ m^{-2}. On the other hand, a radiation-enhanced diffusion coefficient of $D_{\mathrm{rad}}/K = 2 \times 10^{-17}$ m^2/dpa at the same temperature was measured [3]. Since $k_c^2 D_{\mathrm{rad}}/K = 3.8 \times 10^{-3}$ the two measurements are compatible with respect to Eq. (7). The effective production rate η^* of transporting vacancies is limited according to Eq. (7). Using $k_{\mathrm{max}}^2 = 10^{15}$ m^{-2} as a representative value for the effective sink strength (cf. Fig. 7), $10^{-2} < \eta^* < 2 \times 10^{-2}$ is derived, which is compatible with the lower temperature values of the effective fraction η of transporting defects shown in Fig. 7.

Considerably higher swelling rates of 5%/dpa have been reported for a neutron irradiation of nickel at about 570 K with a displacement rate of 6×10^{-10} dpa/s [23]. The sink strength of the voids was estimated to be $k_c^2 = 2 \times 10^{14}$ m^{-2}. Since the diffusion coefficient at this low temperature is $D_{\mathrm{rad}}/K \approx 10^{-18}$ m^2/dpa [3] Eq. (7) fails in this case indicating that most of the swelling is caused by vacancies which do not significantly contribute to diffusion, i.e., by diffusing vacancy clusters. As has been stated already earlier [4,5,12,20,24], a meaningful comparison of swelling and diffusion measurements is only possible when the contribution of different mobile defect species, i.e., single defects and clusters, to the radiation effect is considered in detail. In this respect it is emphasized again that diffusion measurements are mainly sensitive to the actual concentration of mobile single defects. Therefore, the fractions of transporting defects η deduced from the present investigation are only part of the migrating defect fraction (MDF) defined elsewhere [24]. They are, however, the important part for the radiation-enhanced atom transport phenomena.

5. Summary

The fundamental parameters effective fraction η of transporting defects and effective sink strength k_{max}^2 for energetic ion irradiation have been evaluated by analyzing the depth dependence of the radiation-enhanced diffusion coefficient near the irradiated surface of pure nickel. Fractions η of 0.7% to 3% of the displacement rate, and effective sink strength k_{max}^2 of 10^{15} to 3×10^{15} m^{-2} are deduced for noble gas irradiations at 800 and 950 K. Self-ion irradiation yields $\eta = 2\%$ and $k_{\mathrm{max}}^2 = 10^{15}$ m^{-2} at 890 K, and $\eta = 7\%$ and $k_{\mathrm{max}}^2 = 3 \times 10^{14}$ m^{-2} at 950 K. The radiation-induced sink strength under noble gas irradiation at 950 K increases with increasing displacement rate. Generally, with increasing temperature the sink strength decreases while the effective fraction of transporting defects increases.

Acknowledgements

Valuable suggestions and helpful comments by Dr C. Abromeit and Dr H. Trinkaus are gratefully acknowledged. We thank Mrs I. Dencks, D. Köpnick, C. Weimann, and D. Yaraghchi for the careful preparation of the multi-layer specimens.

References

[1] R. Sizmann, J. Nucl. Mater. 69&70 (1978) 386.
[2] Y.-T. Cheng, Mater. Sci. Rep. 5 (1990) 47.
[3] A. Müller, V. Naundorf, M.-P. Macht, J. Appl. Phys. 64 (1988) 3445.
[4] H. Trinkaus, V. Naundorf, B.N. Singh, C.H. Woo, J. Nucl. Mater. 210 (1994) 244.
[5] V. Naundorf, H. Wollenberger, J. Nucl. Mater. 212–215 (1994) 226.
[6] L.E. Rehn, P.R. Okamoto, R.S. Averback, Phys. Rev. B30 (1984) 3073.
[7] H. Wollenberger, in: Physical Metallurgy, ed. R.W. Cahn and P. Haasen (Elsevier, Amsterdam, 1996) p. 1621.
[8] G. Neumann, in: Diffusion in Solid Metals and Alloys, ed. H. Mehrer, Landold-Börnstein, New Series III/26 (Springer, Berlin, 1990) p. 183.

[9] J.P. Biersack, L.G. Haggmark, Nucl. Instrum. Meth. 174 (1980) 257.
[10] Neutron Radiation Damage Simulation by Charged Particle Simulation, Report No. ASTM E 521-89 (American Society for Testing and Materials, Philadelphia, PA, 1989) p. 167.
[11] M.-P. Macht, R. Willeke, V. Naundorf, Nucl. Instrum. Meth. 43 (1989) 507.
[12] W. Schilling, H. Ullmaier, in: Materials Science and Technology, Vol. 10, ed. R.W. Cahn and P. Haasen (VCH, Weinheim, 1993) p. 179.
[13] A.D. Brailsford, R. Bullough, Philos. Trans. R. 302 (1981) 87.
[14] M.A. Kirk, J.M. Robertson, M.L. Jenkins, C.A. English, T.J. Black, J.S. Vetrano, J. Nucl. Mater. 149 (1987) 21.
[15] S. Ishino, N. Sekimura, H. Sakaida, Y. Kanzaki, Mater. Sci. Forum 97–99 (1992) 21.
[16] J. Tenbrink, R.P. Wahi, H. Wollenberger, in: Effects of Radiation on Materials: 14th Int. Symp., Vol. 1, ed. N.H. Packan, R.E. Stoller and A.S. Kumar, ASTM STP 1046 (American Society for Testing and Materials, Philadelphia, PA, 1989) p. 543.
[17] J. Rest, R.C. Birtcher, J. Nucl. Mater. 168 (1989) 312.
[18] T. Ezawa, M. Sugimoto, K. Niwase, S. Sasaki, A. Iwase, T. Iwata, F.E. Fujita, J. Nucl. Mater. 179–181 (1991) 974.
[19] K. Niwase, T. Ezawa, T. Tanabe, M. Kiritani, F.E. Fujita, J. Nucl. Mater. 203 (1993) 56.
[20] H. Trinkaus, B.N. Singh, A.J.E. Foreman, J. Nucl. Mater. 199 (1992) 1.
[21] J.E. Westmoreland, J.A. Sprague, F.A. Smid Jr., P.R. Malmberg, Radiat. Eff. 26 (1975) 1.
[22] B.N. Singh, S.I. Golubov, H. Trinkaus, A. Serra, Yu.N. Osetzky, A.V. Barashev, these Proceedings, p. 107.
[23] M. Kiritani, T. Yoshiie, S. Kojima, Y. Satoh, K. Hamada, J. Nucl. Mater. 174 (1990) 327.
[24] S.J. Zinkle, B.N. Singh, J. Nucl. Mater. 199 (1993) 173.